Numerical Methods in Civil Engineering

Using FEM to achieve acceptance criteria in FEMA performance levels for FRP-wrapped RC circular columns

Seyed Bahram Beheshti Aval*, Mohammad Parsaei**

ARTICLE INFO

Article history:
Received:
January 2019.
Revised:
April 2019.
Accepted:
May 2019.

Keywords:
Finite Element Analysis;
Fiber Reinforced Polymer;
Bridge Pier;
Strengthening;
Plastic Hinge Rotation Angle

Abstract:

Using fiber reinforced Polymer composite materials (FRP) in the rehabilitation schemes of vulnerable structural members is becoming more popular over the past decades. From the analytical point of view, the lack of numerical acceptance criteria in attaining the desired performance goal is a major restriction in employing this retrofitting method. The major parameter to control the seismic performance of frame members in nonlinear behavior is plastic hinge rotation angle (PHRA) especially for deformation-controlled actions. To predict accurate performance of RC columns, strengthened with externally-bonded FRP, there is an urgent need to discover PHRA as the acceptance criteria in a nonlinear static procedure stipulated in ASCE/SEI 41-13 standard. As indicated, the parameters such as FRP thickness to section diameter ratio (aspect ratio), the relative height of FRP and the FRP material properties have significant influence on the behavior of the members strengthened with FRP under combineed cyclic axial-flexural loading. For easy use, analytical formulation is calibrated to evaluate PHRA as the function of the aforementioned triple parameters. An attempt has been made to simulate the RC columns with FRP laminate with general-purpose finite element software ABAQUS. Verification of the numerical method has been done by comparing numerical results versus existing experimental tests.

1. Introduction

Today many reinforced concrete (RC) bridges under operation are vulnerable or damaged by natural disasters such as earthquake, wind, fatigue due to service loads, and corrosive environment. A lot of old bridges that have been designed based on linear analytical models are vulnerable to strong earthquake ground motions. If it is confirmed that these structures are ineligible to fulfill selective performance level, one or more elements may be needed to retrofit or substitute. The required performance level should be supplied by a rehabilitation scheme. Replacing the deficient members with new ones from economic and practical view point is not feasible, whilst repair and strengthening is essential and cost effective.

**Corresponding Author: Associate Professor, Faculty of Civil Engineering, K. N. Toosi University of Technology, Tehran, Iran. E-mail: beheshti@kntu.ac.ir*

***Structural Engineer, former M.Sc. student graduated at Faculty of Technical and Engineering, Science & Culture University, Tehran, Iran,*

Currently various methods are utilized for repairing and retrofitting of RC structures. Among them steel and RC jacketing are popular between engineers specially for members under compression loads. In comparison with RC jacket, steel jacketing has the advantage of lighter weight [1,2]. However, application of steel has several shortcomings such as hard labor, higher cost, and vulnerability from corrosive environment. In comparison with steel jacketing, Fiber Reinforced Polymer (FRP) laminate has some advantages such as easy to use, higher resistance to corrosive environment, and also augmented stiffness and strength. Due to these excellences, this material has attracted the attention of more and more engineers. In recent decades FRP is widely used to repair and retrofit RC structures. Recent study shows high performance of this technique especially in confinement of RC compression members [3,4]. Among columns with various geometrical section configurations, circular ones are very susceptible to strengthening due to uniform confinement received by FRP wrapping [5-9]. Confinement by transverse reinforcement and its effect on strength and

ductility are classical concepts in design of RC columns. Obviously, the confinement from transverse reinforcement causes an increase in compressive strain capacity and therefore improvement in ductility. Improvement of strain capacity from FRP confinement is noticeable [10,11]. The results of previous experimental and analytical studies showed that encasing circular columns with FRP laminate caused a uniform confinement. Various analytical models have been suggested for circular sections in technical literatures [12]. The confinement level depends on strength, type, and aspect ratio (column diameter to FRP thickness). The confinement effect is maintained until FRP's tensile and compressive strength reaches its ultimate values [13].

Usually seismic rehabilitation standards introduce quantitative acceptance criteria for performance levels regarding member behavior under seismic actions. Based on state of the knowledge, acceptance criteria of flexural RC members in each performance level is controlled by ductility parameters such as value of plastic hinge rotation angle (PHRA). Perhaps one of the challenges in the widespread use of FRP for retrofitting of RC members is restricted knowledge of the parameters affecting the post-elastic behavior of the strengthening of RC members [14]. Results of carried out experimental and analytical studies showed preferable use of this material in nonlinear range of behavior. With Reference to the above mentioned advantages, applicability of FRP for these deficient bridges are more and more widespread. Damages reported to these structures from strong ground movement are plastic flexural hinge formed at the fixed ends of piers. Inadequate confinement in plastic flexural hinge length causes pulling out and buckling of longitudinal rods between transverse shear reinforcements. Hitherto no acceptance criteria of performance levels for RC members strengthened with FRP has been provided by corresponding documents. In this study, the main impressive parameters for confinement of members with FRP such as FRP thickness to section diameter ratio (aspect ratio), the relative height of FRP and the FRP material properties are used to predict PHRA capacity in each performance level. To predict the performance of fiber-wrapped concrete columns accurately, there is an urgent need to discover the required parameters for model and acceptance criteria in a nonlinear static procedure stipulated in ASCE/SEI 41-13 [15] standard.

Numerous attempts have been made to introduce analytical closed form expressions to estimate acceptance criteria for beam-column elements under axial-flexure loading [16-19]. However, they presented the strength and ductility in ultimate limit state and have not yet provided the criteria at least in the major performance levels i.e. Immediate Occupancy (IO), Life Safety (LS), and Collapse Prevention (CP), which are introduced in the performance based design guidelines.

In this study an effort has been made to simulate the RC piers strengthened with FRP laminate with a suitable finite element program. Along with evaluation of PHRA, the plastic hinge length should also be calculated. So the flexural hinge length followed by the optimal FRP length from pier's fixed end are introduced. Due to unavailable laboratory results on cyclic behavior of RC piers with various length of FRP wrapping and other effective parameters under axial-flexural loading, the development of the reliable finite element models verified versus existing experimental results seems necessary.

2. Finite Element Model

An establishment of an accurate and reliable 3D finite element model is an essential step in numerical simulation of structures under applied forces. Each material type of circular column including externally bonded FRP, steel reinforcing, and concrete should be modeled with appropriate element type. To this end, general-purpose FEM software ABAQUS [20], which has a complete element library specially including superior concrete model with capability of elastic-plastic damage behavior was utilized here.

2.1. Concrete

Concrete is modeled by the damaged plastic behavior. This model is capable of behaving accurately under monotonic as well as cyclic loads. Introducing accurate compression and tensile stress-strain concrete behavior to the software causes close results to the achieved experimental evidences. The eight-node isoparametric elements are used to model three-dimensional behavior of concrete.

2.2. Reinforcing Steel

Three dimensional truss elements are used to model transverse and longitudinal reinforcements. These elements are able to model yielding behavior of reinforcement. The reinforcement and concrete are defined in the same phase.

2.3. FRP

To model FRP jackets, four-node shell elements are used. The linear elastic behavior up to rupture point is maintained throughout all analyses. As a matter of fact, a perfect bond between FRP and concrete surfaces was considered. When the FRP is fully bonded to concrete while the column is under axial compression, there may be a possibility to exert undesired stress to the FRP in the direction perpendicular to the fibers. In other words, the axial shortening of the column may damage the fibers in their weak direction. For this reason and also to avoid such

unexpected damages to the fibers, the FRPs are not connected to the foundation directly. Hence, like experimental setup, separate nodes are allocated for FRP and concrete at end base in analytical modeling. As a result of including transverse shear deformation for FRP sheet, these elements can model thin as well as thick shells. To prevent shear locking, the reduced integration method was used.

3. Verification of Analytical Model

Development of reliable finite element model to predict precisely the behavior of structural elements seems necessary. The verification of results is one of the most important and essential steps in numerical study, and requires a selection of suitable mesh size in a finite element procedure. This selection especially affected the slope steepness of post-strength part of load-deformation response of RC members [11]. Therefore, it is necessary to choose elements sizes in such a way that the analytical and experimental results have a reasonable agreement. Based on acceptable accuracy, the meshing scheme consists of 32 elements in each section. The analytical results were verified against eight laboratory specimens, where only two samples are presented. For more verification tests, reader is referred to reference No. [13]. These samples which belong to Saadatmanesh and Ehsani [21], encompass ten scaled specimens. These casted samples were similar to common highway bridge piers specs which were built in high seismic risk areas before 1971. The sample shown in Fig.1 has 2410 mm height and 305 mm diameter. The column was wrapped with six layers of FRP straps resulting in a total thickness of 5 mm and 635 mm length from the bottom. The unidirectional tapes of E-glass were embedded in straps. The analytical results versus laboratory ones are depicted in Fig. 2. Reasonable conformity can be observed between the results. This shows the reasonable accuracy of model used throughout this study.

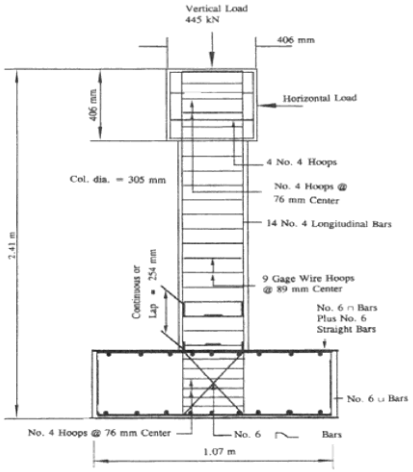

Fig. 1: Side view of test specimen [21]

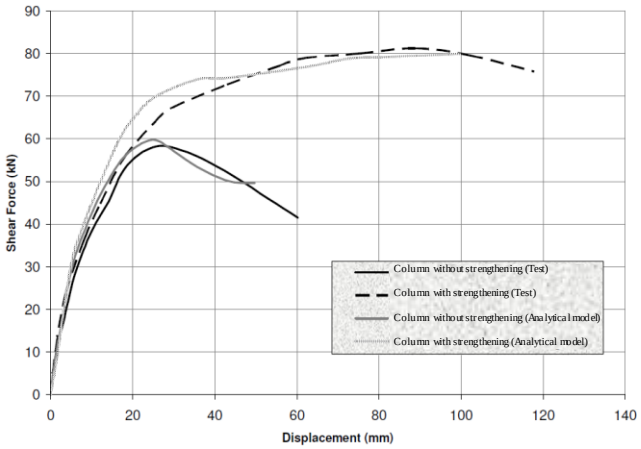

Fig. 2: Comparison of base shear-top displacement (analytical vs. tests)

4. Numerical study

4.1. The Model Specifications

In this section, results of numerical study on the RC columns strengthened with FRP are illustrated. The test setup is represented similar to Fig. 1. The axial load that is applied first, simulates gravity load and was maintained constant throughout the analysis. The monotonic lateral displacement was then applied at the top. The geometric and material properties and axial loads for tested specimens are summarized in Table 1, where N is applied axial load, N_0 is column axial load capacity, calculated by $N_0 = 0.85 f_c' A_g + f_y A_s$, D is outer diameter of circular section, t is FRP thickness, L is column height, f_c' is compressive strength of concrete, d_b and d_c are longitudinal and transverse reinforcement rebar diameter respectively, f_y is yield strength of steel, and "i" is FRP length to column height ratio. FRC and FRG denote carbon and glass fiber respectively. Similar to verification samples, the columns were wrapped with unidirectional tapes embedded in straps. It is assumed that while stress passes ultimate value, rupture occurs in the steel bars. The rupture strains for GFRP and CFRP are assumed to be 0.005 and 0.002 respectively. These values are considered below the actual rupture strain of FRP materials. Such lower values might be acceptable because wrapping FRP material around a curved surface exerts some additional stress which cannot be seen during the material coupon test in the laboratory. Also young modulus for GFRP and CFRP are assumed 53.4 and 173 GPa respectively.

Table 1: Properties of specimens for the case study

Test	N/N_0	*Cover* (*mm*)	L/D	f'_c (*MPa*)	d_b (*mm*)	f_{yL} (*MPa*)	f_{suL} (*MPa*)
C-FRG-i	0.1	25	5	34.5	19.1	303	482
C-FRC-i	0.1	25	5	34.5	19.1	303	482

4.2. Influence of FRP on Plastic Hinge Length and Plastic Hinge Rotation Capacity

Our first attempt is the optimal FRP length for deficient RC piers and then, a comprehensive parametric study is examined to explore the influence of major parameters such as FRP length, type, and thickness on PHRA capacity of retrofitted RC column. Relative FRP lengths are varied from 0.1 to 0.35 and aspect ratios from 133 to 800. The graphs of moment-curvatures for various CFRP/GFRP lengths and aspect ratios are shown in Fig. 3-4.

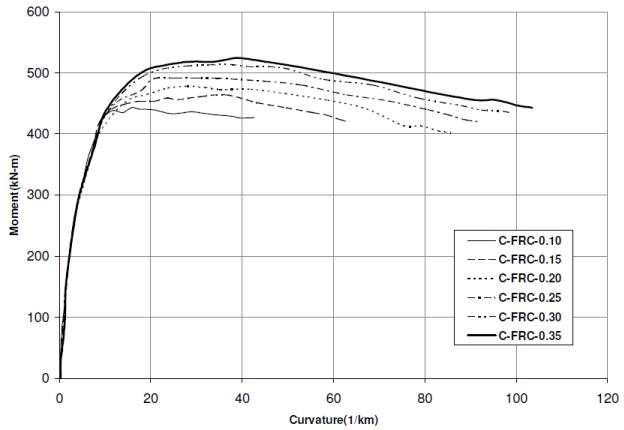

(a) CFRP

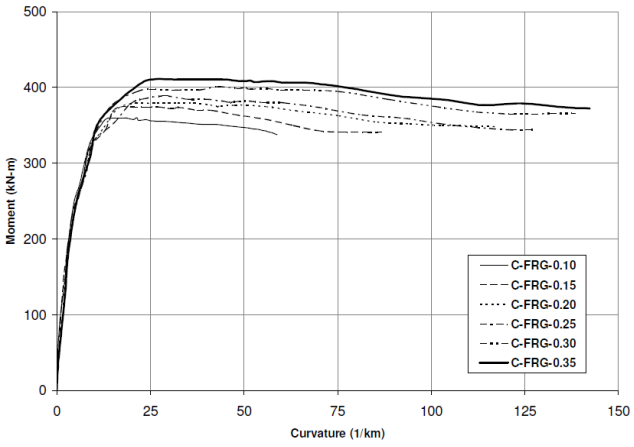

(b) GFRP

Fig. 3: Moment-Curvature relationship of retrofitted pier section for various relative FRP length

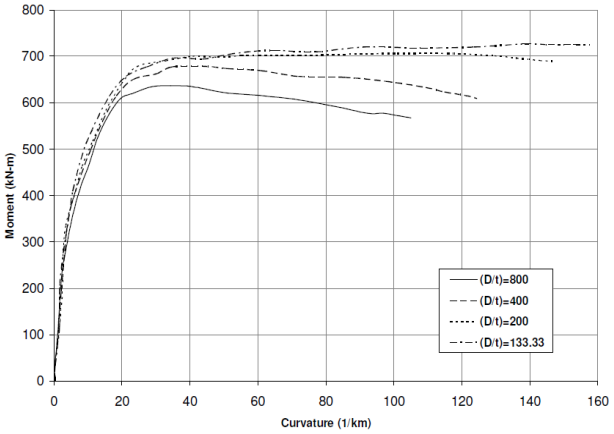

(a) CFRP

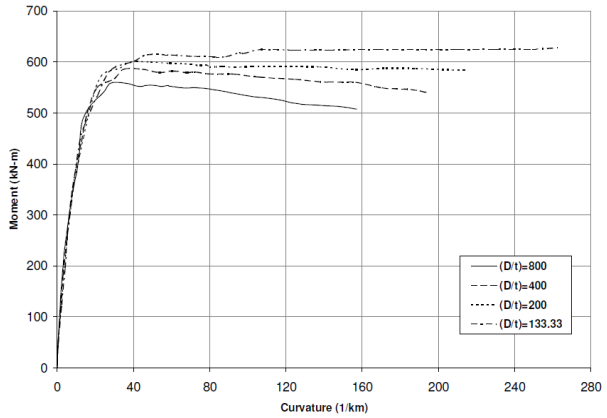

(b) GFRP

Fig. 4: Moment-Curvature relationship of retrofitted pier section for various FRP thickness

Due to the possible occurrence of plastic hinge at the end of the piers, adequate ductility should be provided at that region in high seismic risk areas. One of the major influential factors on inelastic deformation capacity without any failure is lateral confinement. Implementation of FRP encasement enables to provide adequate confinement for this purpose.

Referring to Fig. 5, to capture plastic hinge length, the ultimate and yield curvatures of the retrofitted section are required to be defined. Ultimate curvature is calculated based on concrete compression failure, bar cut off, or FRP fracture, depending on where damage is first. When the outer tension steel bar at the section yielded, its curvature reached the yield value. It is assumed that along plastic hinge length, the plastic curvature remains invariable. As can be seen in Fig. 5, the plastic hinge length calculated is based on length between yield section and pier bottom at the onset of the failure. Tension stress monitoring in rebar during analysis can capture the place and time of occurrence of yielding. Plastic rotation angle may be

estimated as:

$$\theta_i = \int_{l_1}^{l_2} \phi \, dl \rightarrow \theta_p = \int_0^{L_p} \phi \, dl = (\phi_u - \phi_y) \times L_p$$

$$\rightarrow \theta_p = \phi_p L_p \qquad (1)$$

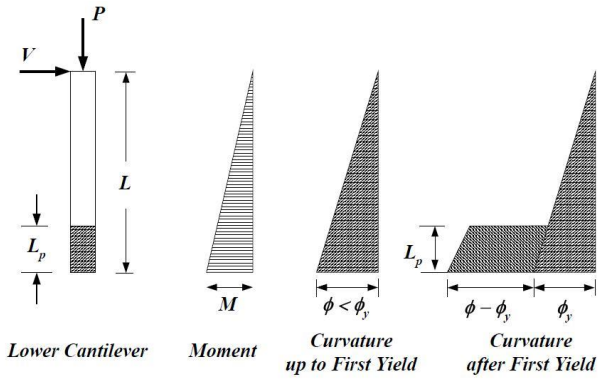

Fig. 5: Moment and curvature for a RC pier.

The plastic hinge length and plastic hinge rotation for columns with various FRP lengths and thicknesses are evaluated and shown in Fig. 6 -7. These Figs show that increasing FRP length (from relative length of 0 to 0.35) causes an increase in plastic hinge length. This augmentation for CFRP is about 7% and for GFRP, it is about 5%. In comparison with GFRP, CFRP has more influence on plastic hinge length. Regarding Fig. 6, although the increasing of FRP length causes the increase of plastic hinge rotation capacity, the growing rate of the plastic hinge rotation gets much slower in the range of relative FRP height of 0.3 to 0.35. For GFRP, a decrease in plastic hinge rotation may be seen.

Fig. 7 shows the influence of FRP thickness on the length and rotation of plastic hinge. For less thickness (less than 1 mm thick), both FRP types have almost equal impact on increasing plastic hinge length. However, increasing FRP thickness has more influence on pier reinforced with carbon composite in comparison with glass ones and has almost the same effect on plastic rotation capacity for both types.

As a whole, the comparison of results in Figs 6-7 shows that although increase of the relative FRP length above 0.35 causes the plastic hinge length to be somehow increased, it may hardly have any effect on the plastic hinge length at all. Hence, FRP length of (0.3-0.35) L is a good choice for CFRP as well as GFRP type.

For verification, these results are compared with the results of Seible et al. [22]. Based on their studies, the FRP length is evaluated as:

$$L_c = L_{c1} + L_{c2} \qquad (2)$$

where,

L_{c1} = primary confinement region for plastic hinge;

L_{c2} = secondary confinement region adjacent to plastic hinge

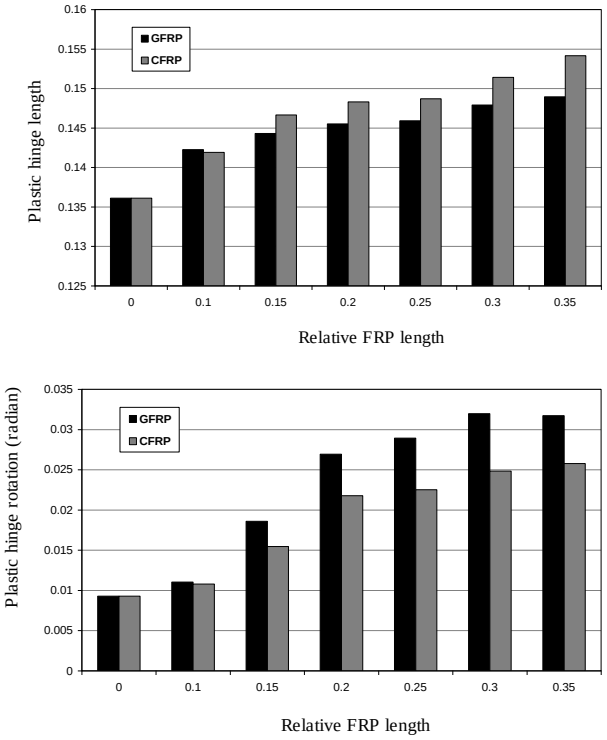

Fig. 6: Plastic hinge length and plastic hinge rotation vs. relative FRP length for GFRP and CFRP

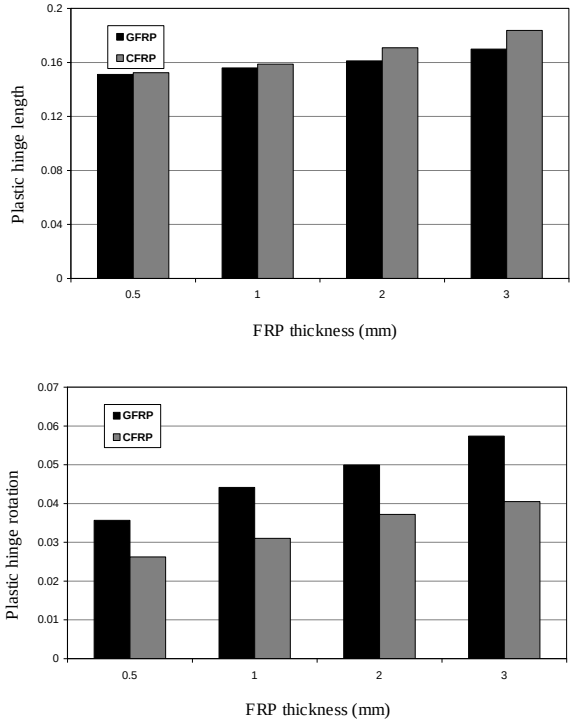

Fig. 7: Plastic hinge length and plastic hinge rotation vs. FRP thickness for GFRP and CFRP

The secondary confinement region is necessary to prevent occurrence of flexural plastic hinge above the primary plastic hinge length when confinement allows for significant over strength development in the primary plastic hinge. Plastic hinge confinement lengths L_{c1} and L_{c2} are related to the column geometry based on the expected plastic hinge length, both in terms of column depth/diameter in the loading direction, and to the shear span or distance from the column hinge to the point of contraflexure. It is recommended:

$$L_{c1} \geq \begin{cases} L_P \\ 0.5d \\ L/B \end{cases} \quad , \quad L_{c2} \geq \begin{cases} L_P \\ 0.5d \\ L/B \end{cases} \tag{3}$$

Where,

L_p =plastic hinge length

d = column diameter

L =column height

B =column width for rectangular sections

Referring to Park's proposal [23], the plastic hinge length of RC column is:

$$L_P = 0.08L + 0.022 f_y d_b \tag{4}$$

L =column height in millimeter (between maximum and zero moment)

f_y = yield stress of longitudinal reinforcement in MPa

d_b = diameter of longitudinal reinforcement

Based on Binici and Mosalam [24], the plastic hinge length considering confinement effect is

$$L_P = 0.077L + 8.16d_b \tag{5}$$

From equations (2) and (5), the FRP strengthening length would be:

$$L_p = 0.077 \times 2000 + 8.16 \times 19.1 = 309.856 \ mm$$

$$L_{c1} \geq \begin{cases} L_P = 309.856 \\ 0.5d = 0.5 \times 400 = 200 \end{cases} \quad , \quad L_{c2} \geq \begin{cases} L_P = 309.856 \\ 0.5d = 0.5 \times 400 = 200 \end{cases}$$

$$L_{c1} \geq 309.856 \qquad L_{c2} \geq 309.856$$

$$L_c = L_{c1} + L_{c2} = 309.856 + 309.856 = 619.712 \ mm$$

For this 2-meter column, the length which is equivalent to (0.309L), can be seen to have a negligible difference, with the proposed analytical model (0.3-0.35L).

5. Plastic hinge proposal for each performance levels

In nonlinear range of deformation, deflections of piers are dominated by plastic hinge rotation [25]. Although there are numerical acceptance criteria for nonlinear procedures of RC columns for triple performance levels in ASCE/SEI 41-13 [15], the reader could not find the similar parameters for RC sections confined by FRP. Table 10-8 of that standard shows the plastic hinge rotations capacity for RC Columns in each selected performance level. These values depend on several parameters i.e. axial and shear force levels, inadequate development or splices of longitudinal reinforcements.

It appears that introducing plastic hinge rotation capacity for pier sections confined by FRP can lead to more applicability of this document for the strengthening scheme. Using energy based concept is a good tool to establish these values for selected performance levels.

6. Energy Based Method to Determine Plastic Hinge Rotation in Each Performance Levels

Defining vulnerability description for each performance levels of piers retrofitted by FRP needs extensive data from previous earthquakes and experimental tests. This technology has recently become popular in strengthening of existing buildings. Because of limited available test data, accurate analytical modeling seems the second chance to evaluate acceptance criteria for these types of structures. The finite element method is a good tool to elaborate this purpose.

In this way, based on evaluated maximum plastic hinge rotation onset of failure of pier from analytical model, the amount of plastic rotation at level of collapse performance is computable. This rotation is denoted by $\theta_{CP'}$. The subscript prime stands for samples strengthened with FRP. To find criterions for other performance levels (IO, LS), a simple assumption may be considered as the ratio of absorbed energy for the pair of performance levels preserved for piers with and without FRP. For instance, in order to find a criterion for plastic rotation in immediate occupancy performance level, the ratio of absorbed energy for CP and IO performance level is considered equal to pier with and without FRP laminates. Although strengthening with FRP causes a significant absorbed energy from IO to CP level, in comparison with RC piers, preserving this ratio for two piers according to equation 6, causes a conservative value for plastic hinge rotation in IO level of FRP pier. Having plastic rotations for IO and CP levels from Table 10-8 of ASCE/SEI 41-13 [15] for RC piers and plastic rotation in onset of collapse from analytical modeling, the plastic rotation in IO level for FRP pier could be computed from the following equality:

$$\frac{E_{IO'}}{E_{IO}} = \frac{E_{CP'}}{E_{CP}} \tag{6}$$

The same methodology could be used for LS performance level. So the plastic rotation in IO level for FRP pier could be computed from the following equality:

$$\frac{E_{LS'}}{E_{LS}} = \frac{E_{CP'}}{E_{CP}} \quad (7)$$

For applicability purposes, the introduced formulas that yield plastic rotation in each performance level based on three effective parameters, (i.e. FRP length, thickness, and material type) are necessary. 48 columns with various FRP thickness (0.5, 1, 2, 3 mm) and FRP length (0.1L, 0.15L, 0.2L, 0.25L, 0.3L, 0.35L), from carbon and glass fiber are analyzed. Two results of these analyses (base shear vs. top displacement) for two samples with various material and thickness are shown in Fig. 8. The curvature and plastic rotation at bottom end of pier started at the onset of collapse can be adopted from these diagrams. Each column at table 3-6 is denoted as CX-Y-Z in which X stands for Glass or Carbon fiber, Y for FRP thickness and Z for relative FRP length. Strength and ductility are increased with the increase of thickness and length of FRP. The GFRP and CFRP demonstrate more influence on ductility and strength respectively.

Failure commencement of column may be triggered by one or a combination of the following mechanisms:

1. Longitudinal rebar losing its ability to bear load after outer concrete shell spalling off. The outward buckling is casted in this category.
2. Fracture of lateral reinforcement
3. Fracture of FRP shell.
4. Concrete core crushing loss due to confinement loss.

During analysis, the above criteria are monitored to find out the onset of collapse mechanism of columns. Stress and strain at yielding and failure of steel reinforcement are shown in Fig. 9. Since the behavior of FRP up to failure is considered linear, both the stress and strain can simultaneously reach their ultimate values. These values are presented in Fig. 9. The ultimate curvature and plastic hinge rotation for these 48 columns with various CFRP/GFRP thickness, and length are depicted in Table 2. These values are recognized for CP performance level.

Based on Eqs. 6 and 7 and the amount of plastic hinge rotation in various performance levels for RC column which are depicted in Table 10-8 of ASCE/SEI 41-13 [15], the corresponding plastic hinge rotations for FRP columns are calculated and introduced in Table 3-4 for CFRP and GFRP respectively. Since aspect ratio ($\frac{t}{D}$) and the relative FRP length ($\frac{L_f}{L_c}$) have the same influence on confinement and ductility of column, these values are introduced based on parameter $\frac{L_f \cdot t}{L_c \cdot D}$. Utilizing this parameter is interesting for applicability purposes.

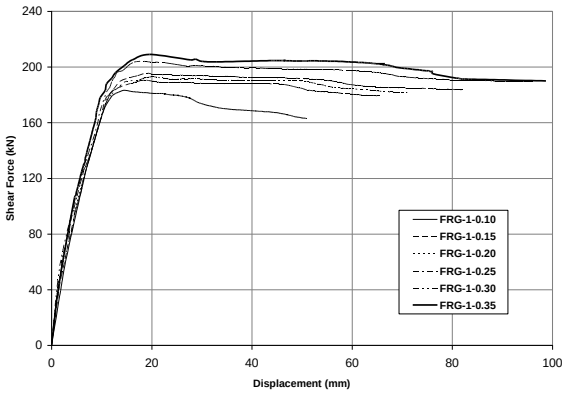

(a) 1 mm GFRP

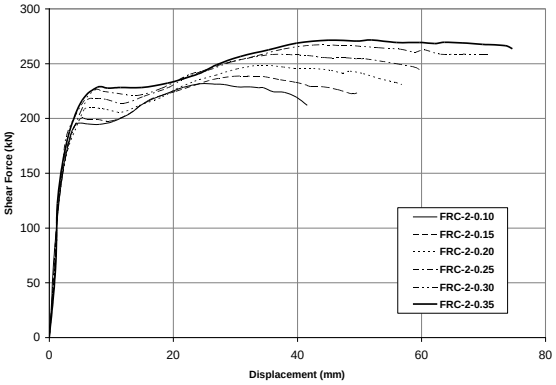

(b) 2 mm CFRP

Fig. 8: Base shear – top displacement of circular column with different FRP thicknesses and materials

A curve fitting is used to find a relationship composed of this combined parameter and plastic hinge rotation in various performance levels. These curves are shown for columns retrofitted with CFRP and GFRP in Fig. 10.

The proposed relation between combined parameter $x = \frac{L_f \cdot t}{L_c \cdot D}$ and plastic hinge rotation $y = \theta'_{PL}$ may be recognized as:

$$y = a + b\,x + cx^2 \quad (8)$$

The coefficients a, b, and c can be obtained from Table 5 at triple performance levels for GFRP and CFRP respectively.

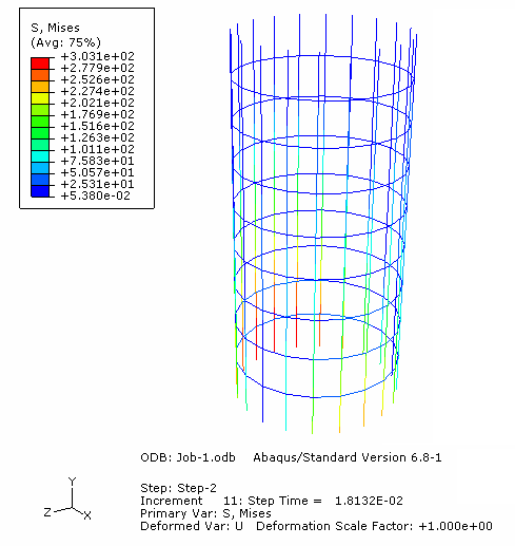

(a) Steel rebar yield stress (f_{sy})

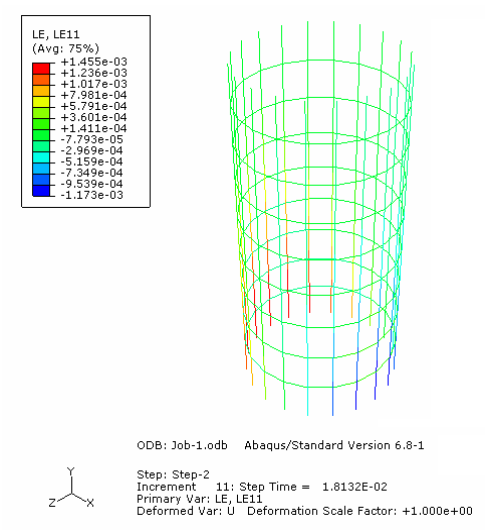

(b) Steel rebar yield strain (ε_{sy})

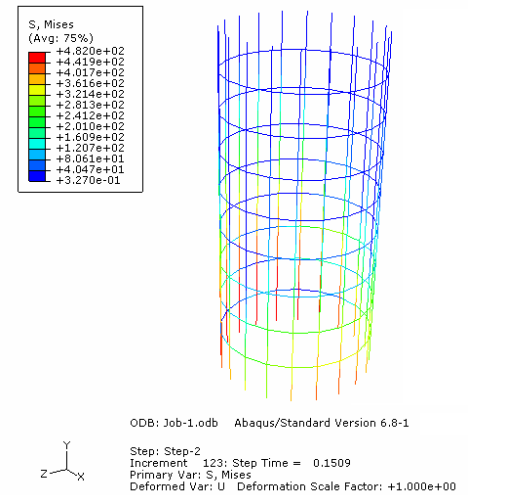

(c) Steel rebar ultimate stress (f_{su})

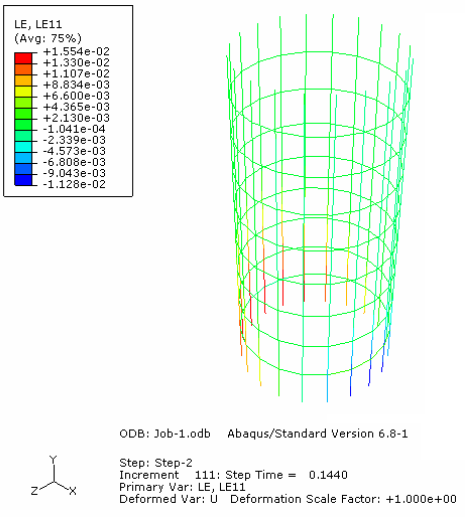

(d) Steel rebar ultimate strain (ε_{su})

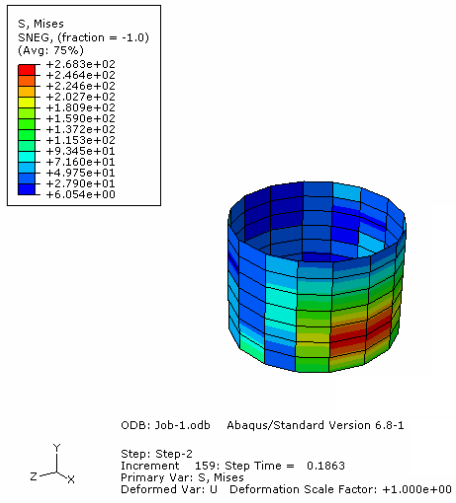

(e) FRP failure stress (f_{frpu})

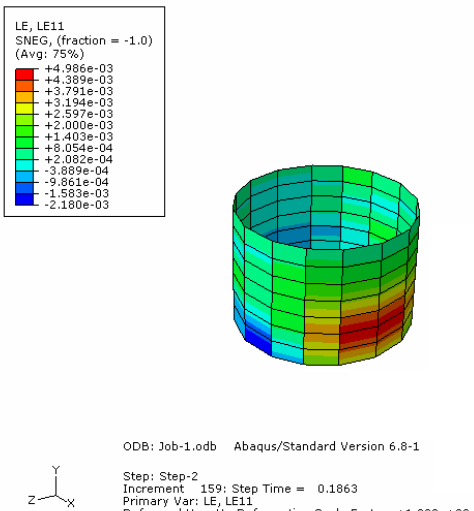

(f) FRP failure strain (ε_{frpu})

Fig. 9: Probable failure mechanism of column

Table 2: Ultimate curvature and plastic hinge rotation for 48 columns with various CFRP/GFRP thickness, and length

	Column	ϕ_u	θ_p
CFRP (0.5 mm thickness)	FRC-0.5-0.10	36.692	0.01025
	FRC-0.5-0.15	54.283	0.01376
	FRC-0.5-0.20	75.171	0.01899
	FRC-0.5-0.25	77.187	0.01995
	FRC-0.5-0.30	87.734	0.02256
	FRC-0.5-0.35	92.152	0.02240
GFRP (0.5 mm thickness)	FRG-0.5-0.10	50.645	0.01021
	FRG -0.5-0.15	75.535	0.01618
	FRG -0.5-0.20	97.921	0.02316
	FRG -0.5-0.25	105.844	0.02445
	FRG -0.5-0.30	116.291	0.02618
	FRG -0.5-0.35	115.551	0.02692
CFRP (1.0 mm thickness)	FRC-1-0.10	42.624	0.01079
	FRC-1-0.15	63.127	0.01546
	FRC-1-0.20	85.670	0.02178
	FRC-1-0.25	91.654	0.02250
	FRC-1-0.30	98.900	0.02484
	FRC-1-0.35	103.480	0.02578
GFRP (1.0 mm thickness)	FRG -1-0.10	58.820	0.01104
	FRG -1-0.15	86.800	0.01858
	FRG -1-0.2	117.800	0.02692
	FRG-1-0.25	127.400	0.02894
	FRG-1-0.30	138.571	0.03197
	FRG-1-0.35	142.281	0.03172
CFRP (2.0 mm thickness)	FRC-2-0.10	48.171	0.01254
	FRC-2-0.15	72.114	0.01828
	FRC-2-0.20	100.265	0.02636
	FRC-2-0.25	105.588	0.02696
	FRC-2-0.30	114.953	0.02909
	FRC-2-0.35	118.458	0.03040
GFRP (2.0 mm thickness)	FRG-2-0.10	60.649	0.01142
	FRG-2-0.15	92.668	0.01990
	FRG-2-0.2	128.146	0.02936
	FRG-2-0.25	137.191	0.03129
	FRG-2-0.30	144.234	0.03484
	FRG-2-0.35	149.176	0.03521
CFRP (3.0 mm thickness)	FRC-3-0.10	53.720	0.01340
	FRC-3-0.15	78.842	0.01880
	FRC-3-0.20	109.678	0.02833
	FRC-3-0.25	118.255	0.02861
	FRC-3-0.30	127.81	0.03187
	FRC-3-0.35	135.521	0.03251
GFRP (3.0 mm thickness)	FRG-3-0.10	70.366	0.02191
	FRG-3-0.15	106.432	0.02228
	FRG-3-0.2	148.677	0.03347
	FRG-3-0.25	156.213	0.03472
	FRG-3-0.30	170.227	0.04007
	FRG-3-0.35	172.971	0.03998

The suggested Eq. 8 can be used as acceptance criteria in nonlinear procedure for RC piers retrofitted with FRP laminate. The combined parameter used in this equation includes the confinement due to secondary parameters i.e. FRP aspect ratio and FRP relative height which are suggested by other researchers.

Table 3: Plastic hinge rotation of GFRP columns for IO, LS, and CP performance level

	Column	$\frac{L_f \cdot t}{L_c \cdot D}$	θ'_{IO}	θ'_{LS}	θ'_{CP}
GFRP (0.5 mm thickness)	CG-0.5-0.10	0.0001250	0.00255	0.00766	0.01021
	CG-0.5-0.15	0.0001875	0.00405	0.01214	0.01618
	CG-0.5-0.20	0.0002500	0.00579	0.01737	0.02316
	CG-0.5-0.25	0.0003125	0.00611	0.01834	0.02445
	CG-0.5-0.30	0.0003750	0.00655	0.01964	0.02618
	CG-0.5-0.35	0.0004375	0.00673	0.02019	0.02692
GFRP (1.0 mm thickness)	CG-1-0.10	0.0002500	0.00276	0.00828	0.01104
	CG-1-0.15	0.0003750	0.00465	0.01394	0.01858
	CG-1-0.2	0.0005000	0.00673	0.02019	0.02692
	CG-1-0.25	0.0006250	0.00724	0.02171	0.02894
	CG-1-0.30	0.0007500	0.00799	0.02398	0.03197
	CG-1-0.35	0.0008750	0.00793	0.02379	0.03172
GFRP (2.0 mm thickness)	CG-2-0.10	0.00050	0.00286	0.00857	0.01142
	CG-2-0.15	0.00075	0.00498	0.01493	0.01990
	CG-2-0.2	0.00100	0.00734	0.02202	0.02936
	CG-2-0.25	0.00125	0.00782	0.02347	0.03129
	CG-2-0.30	0.00150	0.00871	0.02613	0.03484
	CG-2-0.35	0.00175	0.00880	0.02641	0.03521
GFRP (3.0 mm thickness)	CG-3-0.10	0.000750	0.00323	0.00968	0.01291
	CG-3-0.15	0.001125	0.00557	0.01671	0.02228
	CG-3-0.2	0.001500	0.00837	0.02510	0.03347
	CG-3-0.25	0.001875	0.00868	0.02604	0.03472
	CG-3-0.30	0.002250	0.01002	0.03005	0.04007
	CG-3-0.35	0.002625	0.01000	0.02999	0.03998

Table 4: Plastic hinge rotation of CFRP columns for IO, LS, and CP performance level

	Column	$\frac{L_f \cdot t}{L_c \cdot D}$	θ'_{IO}	θ'_{LS}	θ'_{CP}
CFRP (0.5 mm thickness)	CC-0.5-0.10	0.0001250	0.00256	0.00769	0.01025
	CC-0.5-0.15	0.0001875	0.00344	0.01032	0.01376
	CC-0.5-0.20	0.0002500	0.00475	0.01424	0.01899
	CC-0.5-0.25	0.0003125	0.00499	0.01496	0.01995
	CC-0.5-0.30	0.0003750	0.00564	0.01692	0.02256
	CC-0.5-0.35	0.0004375	0.00560	0.01680	0.02240
CFRP (1.0 mm thickness)	CC-1-0.10	0.0002500	0.00270	0.00809	0.01079
	CC-1-0.15	0.0003750	0.00387	0.01160	0.01546
	CC-1-0.20	0.0005000	0.00547	0.01640	0.02178
	CC-1-0.25	0.0006250	0.00563	0.01688	0.02250
	CC-1-0.30	0.0007500	0.00621	0.01863	0.02484
	CC-1-0.35	0.0008750	0.00645	0.01934	0.02578
CFRP (2.0 mm thickness)	CC-2-0.10	0.00050	0.00314	0.00941	0.01254
	CC-2-0.15	0.00075	0.00457	0.01371	0.01828
	CC-2-0.20	0.00100	0.00659	0.01977	0.02636
	CC-2-0.25	0.00125	0.00674	0.02022	0.02696
	CC-2-0.30	0.00150	0.00727	0.02182	0.02909
	CC-2-0.35	0.00175	0.00760	0.02280	0.03040
CFRP (3.0 mm thickness)	CC-3-0.10	0.000750	0.00335	0.01005	0.01340
	CC-3-0.15	0.001125	0.00470	0.01410	0.01880
	CC-3-0.20	0.001500	0.00708	0.02125	0.02833
	CC-3-0.25	0.001875	0.00715	0.02146	0.02861
	CC-3-0.30	0.002250	0.00797	0.02390	0.03187
	CC-3-0.35	0.002625	0.00813	0.02438	0.03251

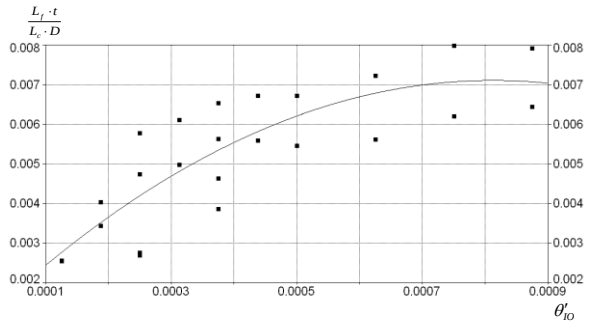

(a) $800 \le D/t \le 400$

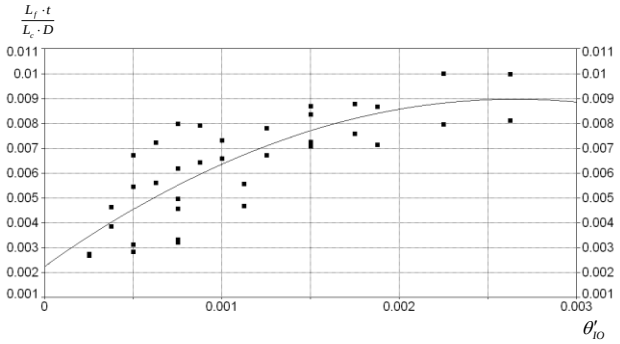

(b) $400 \le D/t \le 133$

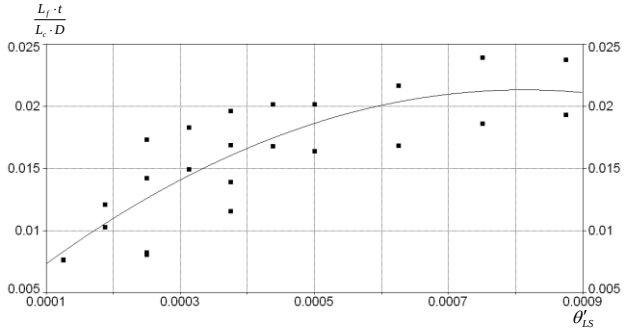

(c) $800 \le D/t \le 400$

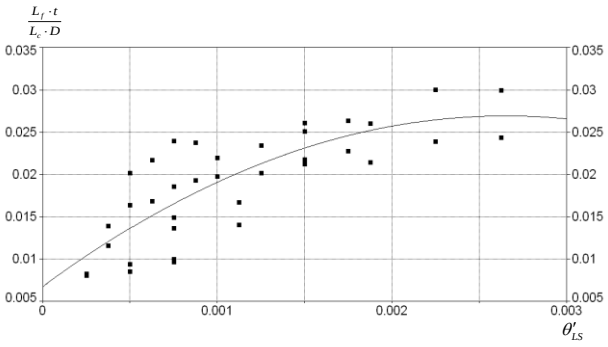

(d) $400 \le D/t \le 133$

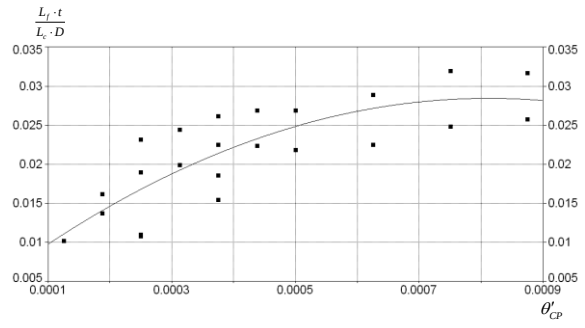

(e) $800 \le D/t \le 400$

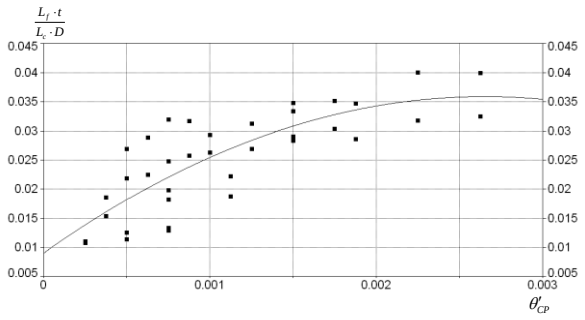

(f) $400 \le D/t \le 133$

Fig. 10: Curve fitting for two ranges of D/t

Table 5: a, b, and c parameters of Eq. 8 for CFRP/GFRP columns at IO, LS, and CP performance level

D/t range		θ'_{IO}	θ'_{LS}	θ'_{CP}
$800 \le D/t \le 400$	*a*	0.00105	0.00314	0.00418
	b	14.9208	44.7625	59.6834
	c	-9176.93	-27530.48	-36707.30
$400 < D/t \le 133$	*a*	0.00225	0.00675	0.00899
	b	5.0732	15.2196	20.2928
	c	-956.41	-2869.23	-3825.64

7. Conclusions

The results of this study and previous experimental tests showed that retrofitting RC columns using FRP wrapping ameliorates their seismic performance characteristics. In the past years, economic factors and the lack of sufficient knowledge limited the use of this technology in the construction industry. However, the decreasing trend of raw materials and manufacturing costs of FRPs have made these materials economically usable in construction building. Another limitation usage of this material is from computational view point. There are no acceptance criteria depicted into rehabilitation documents such as ASCE/SEI 41-13 [15] to check if the desired performance goal is attained. To comply with this goal, an extensive parameter study was performed. 48 columns with various FRP properties up to failure are analyzed. The plastic hinge rotations as acceptance criteria at each performance level are evaluated based on effective parameters such as FRP thickness (aspect ratio), length (relative height) and material kind (glass or carbon fiber). Definition of these acceptance criteria for CP level based on results of collapse analysis are straight forward. To define this criterion for other performance levels (IO, LS), an assured quantity is based on the assumption that the ratio of absorbed energy for a pair of performance levels would be preserved for original and retrofitted column with FRP. Since experimental evidences [26, 27] showed that due to actively FRP-confined concrete, application of FRP can increase the absorbed energy in each performance level in comparison with corresponding RC column. Using this simple assumption leads to the conservative acceptance

criteria for FRP-retrofitted RC pier. As a particular conclusion, the proposed analytical model is capable of anticipating plastic hinge rotation for bridge piers based on FRP parameters at each triple performance levels.

Although transverse reinforcements directly influenced the PHRA and ductility of existing RC columns, and the longitudinal reinforcement indirectly influenced them this paper focused on confinement provided by FRP in a strengthening scheme of deficient RC columns. So throughout this study the same reinforcing steel bars were used for all columns. Undoubtedly, a comprehensive analytical along with experimental effort is required to find a more precise quantity for PHRA capacity of various retrofitted RC columns with different longitudinal and transverse steel reinforcements.

References

[1] Teng, J.G., Xiao, Q. G., Yu, T., Lam, L., "Three-dimensional finite element analysis of reinforced concrete columns with FRP and/or steel confinement", Eng. Struct., vol. 97, 2015, p. 15–28.

[2] Tarabi, A. M., Albakry, F. H., "Strengthening of RC columns by steel angles and strips", Alexandria Engineering, vol. 53, Issue 3, 2014, p. 615-626.

[3] Ozbakkaloglu, T., Xie, T. Y., "Geopolymer concrete-filled FRP tubes: Behavior of circular and square columns under axial compression", Compos. B Eng., vol. 96, 2016, p. 215–230

[4] Mazzucco, G., Salomoni, V., Majorana, C., Pellegrino, C., Ceccato, C., "Numerical investigation of concrete columns with external FRP jackets subjected to axial loads", Constr. Build. Mater., vol. 111, 2016, 590–599.

[5] Paultre, P., M, B. T., Eid, R., and Roy, N., "Behavior of circular reinforced-concrete columns confined with carbon fiber–reinforced polymers under cyclic flexure and constant axial load", *J. of Comp. Constr., ASCE*, vol. 20(3). 2015.

[6] Mostofinejad, D., Moshiri, N., Mortazavi, N., "Effect of corner radius and aspect ratio on compressive behavior of rectangular concrete columns confined with CFRP", Mater. Struct., vol. 48, 2015, p. 107–122.

[7] ID, J. Z., Guo, Y., Li, L. and Chen, W. , "Behavior and Three-Dimensional Finite Element Modeling of Circular Concrete Columns Partially Wrapped with FRP Strips", MDPI, polymers, 2018.

[8] Lin, G., Teng, J. G., "Three-dimensional finite-element analysis of FRP-confined circular concrete columns under eccentric loading", J. Compos. Constr., vol. 21, 2017.

[9] Girgin, Z. C., Girgin, K. A., "design-oriented combined model (7 to 190 MPa) for FRP-confined circular short columns", Polymers, vol. 7, 2015, p. 1905–1917

[10] Hoshikuma, J. Kawashima, K., Nagaya, K., Taylor, A. W., "Stress–strain model for confined reinforced concrete in bridge piers", J. Struct. Eng., ASCE, vol. 123(5), 1997, p. 624-638.

[11] Wu, H.,"Constitutive Model of Concrete Confined by Advanced Fiber Composite Materials and Applications in Seismic Retrofitting", University of Southern California, August 2007.

[12] Hales, T. A., Pantelides, C. P., Reaveley, L. D., "Analytical buckling model for slender FRP-reinforced concrete columns", Composite Structures, vol. 176, 2017, p. 33–42.

[13] Parsaei, M., "The Seismic Behavior of Reinforced Concrete Bridges Pier Retrofitted with FRP", MSc thesis, University of Science and Culture, Faculty of Technical and Engineering, 2009.

[14] Ghanem, S. Y., "Circular RC Columns Partially Confined With FRP", University of Kentucky, PhD Dissertations, Civil Engineering, 2016.

[15] ASCE/SEI 41-13, "Seismic Rehabilitation of Existing Buildings", ASCE, 2013.

[16] ACI 440.2R-17, "Guide for the Design and Construction of Externally Bonded FRP Systems for Strengthening Concrete Structures", Reported by ACI Committee 440, 2017.

[17] AC125, "Acceptance Criteria for Concrete and Reinforced and Unreinforced Masonry Strengthening Using Fiber-Reinforced Polymer (FRP), Composite Systems, 2013.

[18] Monti, G., Alessandri, S., "Design Equations for FRP–Strengthening of Columns", Conference: FRPRCS7, 6-9 November 2005, Kansas City, MO USA, SP-230-60.

[19] Eamonm, C. D., Wu, H. C., Makkawy, A. A., Siavashi, S., "Design and Construction Guidelines for Strengthening Bridges using Fiber Reinforced Polymers (FRP)", Michigan Department of Transportation Research Administration 425 West Ottawa Street Lansing MI 48933 MDOT Reference Number: OR10-039 FINAL REPORT September 30, 2014.

[20] ABAQUS Analysis User's Manual version 6.8.1

[21] Saadatmanesh, H., Ehsani, M.R., Jin. L., "Seismic Strengthening of Circular Bridge Pier Models with Fiber Composites", ACI Structural Journal, vol. 93(6), 1996, p. 639-647.

[22] Seible, F., Priestley M. J. N., Hegemier, G. A., Innamorato, D., "Seismic retrofitting of RC columns with continuous carbon fiber jackets", Journal of Composites for Construction, vol. 1(2), 1997, p. 52–62.

[23] Teng, J.G., Chen, J.F., Smith, S.T, Lam, L., "FRP strengthend RC structures", John Wiley & Sons, New York, NY., 2002.

[24] Binici, B., Mosalam, K.M., "Analysis of reinforced concrete columns retrofitted with fiber reinforced polymer lamina", Journal of Composites: Part B 38, 2007, p. 265–276.

[25] Priestley, M. J. N., Seible, F., and Calvi, G. M., "Seismic Design and Retrofit of Bridges", John Wiley & Sons, Inc., New York, 1996.

[26] Ye, L.P., Zhang K., Zhao S.H., and Feng P.," Experimental study on seismic strengthening of RC columns with wrapped CFRP sheets", Construction and Building Materials, 2003, p.499–506, doi:10.1016/S0950-0618(03)00047-3.

[27] Pantelides, C.P., Gergely, J., Reaveley, L.D. And Volnyy, V.A., "Seismic Strengthening of Reinforced Concrete Bridge Pier with FRP Composites, 12WCEE, 2000